An Observational Study of Typhoon Talim over the Northern Part of the South China Sea in July 2023

Junyi He , Q.S. Li , Pak Wai Chan * , C.W. Choy , Betty Mak , C.C. Lam , H.Y. Luo

Posted Date: 9 August 2023

doi: 10.20944/preprints202308.0713.v1

Keywords: typhoon; LIDAR; wind profiler; dropsonde; ocean radar

Article

An Observational Study of Typhoon Talim over the Northern Part of the South China Sea in July 2023

J.Y. He [1], Q.S. Li [1], P.W. Chan [2], C.W. Choy [2], Betty Mak [2], C.C. Lam [2], H.Y. Luo [3] and P.W. Chan [4,*]

[1] City University of Hong Kong, Hong Kong, China
[2] Hong Kong Observatory, Hong Kong, China
[3] Shenzhen Meteorological Service, Shenzhen, China
[4] Hong Kong Observatory, 134A Nathan Road, Kowloon, Hong Kong, China
* Correspondence: pwchan@hko.gov.hk

Abstract: Extensive surface and upper air measurements of a typhoon over the northern part of the South China Sea, namely, Typhoon Talim in July 2023, are documented and analyzed in this paper. A number of features have been observed from the upper air measurements. First, the log law and the power law are found to be appropriate in fitting the wind profiles of the typhoon in the first 1000 m or so above the sea surface. A low level jet is observed in the lower troposphere from the observations of the radar wind profilers. The paper is also novel from the perspectives that the vertical wind profile from a Doppler LIDAR on an offshore platform over the northern part of the South China sea, and that ocean radar data are used to analyze the surface wind observations of a typhoon in the region. The results of this paper would be useful in understanding the structure of tropical cyclones, e.g., in wind engineering applications.

Keywords: typhoon; LIDAR; wind profiler; dropsonde; ocean radar

Introduction

Tropical cyclones often affect the coast of southern China in the summer each year. For instance, in Hong Kong, on average there are around 4 to 7 tropical cyclones affecting the territory in each summer. Observational data of the cyclones have many important applications. The first direct application is the analysis of the location, intensity and structure of the cyclone, e.g., based on the surface observations. The upper air data are also very valuable, not only in studying the structure of the cyclone, but also have important application as in the design of wind load of tall buildings in southern China.

Observational data, especially the upper air ones, are relatively sparse over the northern part of the South China Sea and along the coast of southern China. However, with the deployment of more meteorological equipment in the region, especially the ground-based remote sensing instruments, increasing amount of data have been collected for tropical cyclones over the South China coastal region and the adjacent waters. The instruments include radar wind profilers and light detection and ranging (LIDAR) wind profiler. In particular, LIDAR wind profilers have been deployed in the offshore oil platforms, providing valuable data in the continuous observation of the atmospheric boundary layer inside and around the tropical cyclones. As reported in Hon and Chan (2022), aircraft observation, especially the dropsondes, is also an important source of in situ upper air measurements inside the tropical cyclone.

For the horizontal structure of the tropical cyclone, apart from in situ anemometers and weather stations, ocean radar has been deployed in the region to observe the spatial distributions of the surface winds, enabling an analysis of the wind structure of the tropical cyclone near the sea surface. Such data have not been documented before in the literature.

In the present paper, the observational data of a strong tropical cyclone case, namely, Typhoon Talim, in July 2023 have been analyzed. This is the first time that a wide collection of observational data have been studied extensively, e.g., in the analysis of the vertical wind profiles for wind engineering applications (on topics such as occurrence of low level jets and fitting of vertical wind

Preprints (www.preprints.org) | NOT PEER-REVIEWED | Posted: 9 August 2023 doi:10.20944/preprints202308.0713.v1

profiles by the power and log laws), as well as the documentation of horizontal structure of the surface wind field. It is hoped that the analysis would stimulate further studies of tropical cyclones in the region, such as comparison of numerical weather prediction model results of the structure of the cyclones in comparison with actual observation data.

Life cycle of Talim

Figure 1 shows the provisional best track of Talim. Talim formed as a tropical depression over the seas west of Luzon on the morning of 14 July 2023. It moved southwestwards slowly on that day. Talim turned to move northwestwards steadily across the northern part of the South China Sea on 15 July 2023 and intensified gradually, reaching the strength of severe tropical storm the next morning. It developed into a typhoon on the night of 16 July 2023, reaching its peak intensity the next day with an estimated maximum sustained wind of around 140 km/h near its centre. Talim continued to move northwestwards and made landfall near Zhanjiang, Guangdong on the night of 17 July 2023. Weakening gradually, Talim moved across Leizhou Peninsula and inland Guangxi on 18 July 2023, and finally dissipated over the northern part of Vietnam on the morning of 19 July 2023.

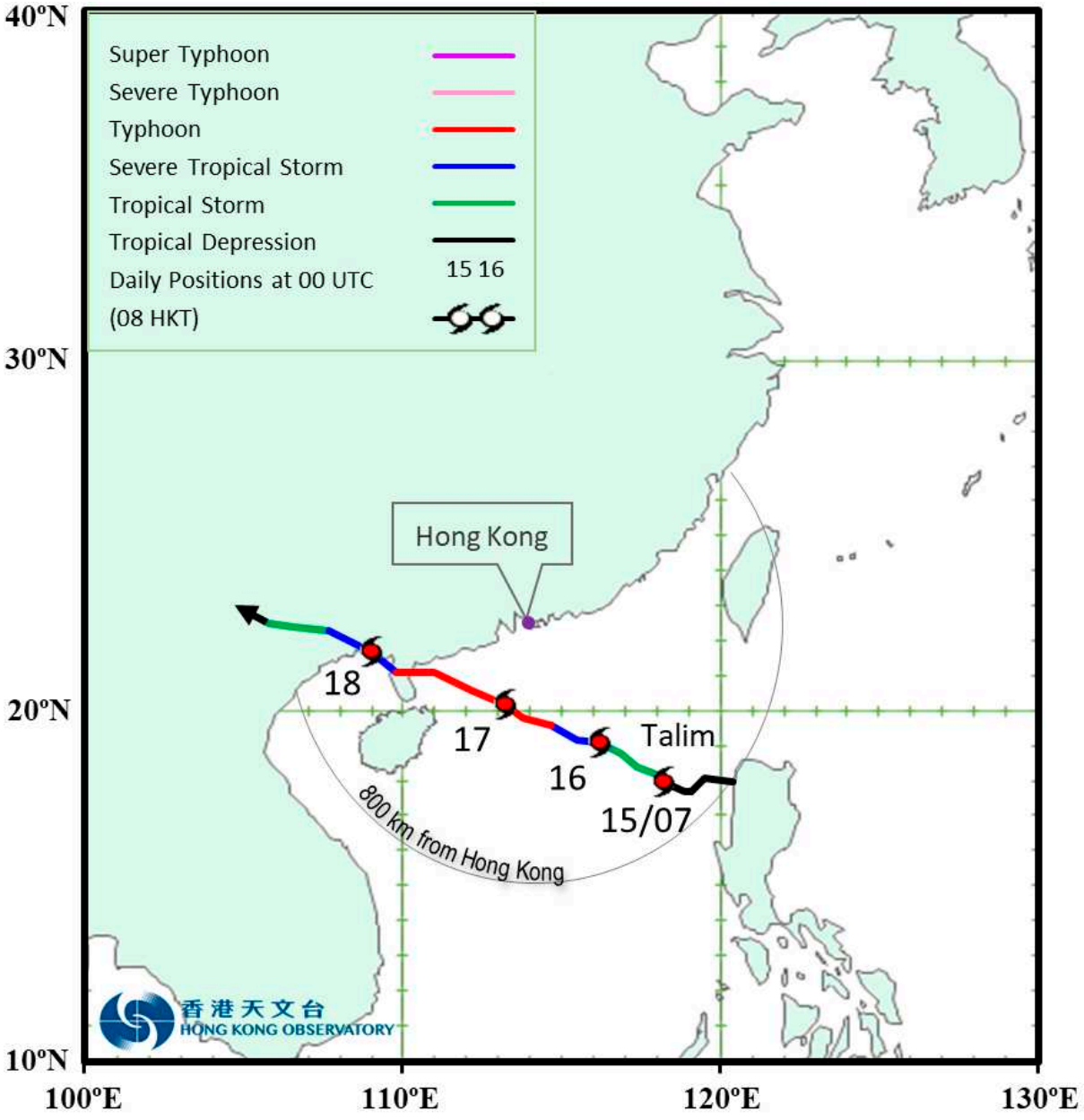

Figure 1. Provisional best track of Talim in July 2023.

Preprints (www.preprints.org) | NOT PEER-REVIEWED | Posted: 9 August 2023 doi:10.20944/preprints202308.0713.v1

Surface and upper air observations

A snapshot of the horizontal distribution of surface wind of Typhoon Talim is given in Figure 2. It could be seen that the gale force wind distribution is rather extensive, with a gale radius in the order of 250 km when Talim was situated to the south of Hong Kong. On a couple of islands and offshore stations, even hurricane force winds in the order of 70 knots (the yellow wind barbs in Figure 2) had been recorded. This is consistent with the dropsonde observations (discussed later) that the near surface wind could reach around 35 m/s. The extensive structure of Talim led to the strengthening of winds over the coastal areas of southern China when the cyclone was still several hundred kilometres away from the coast.

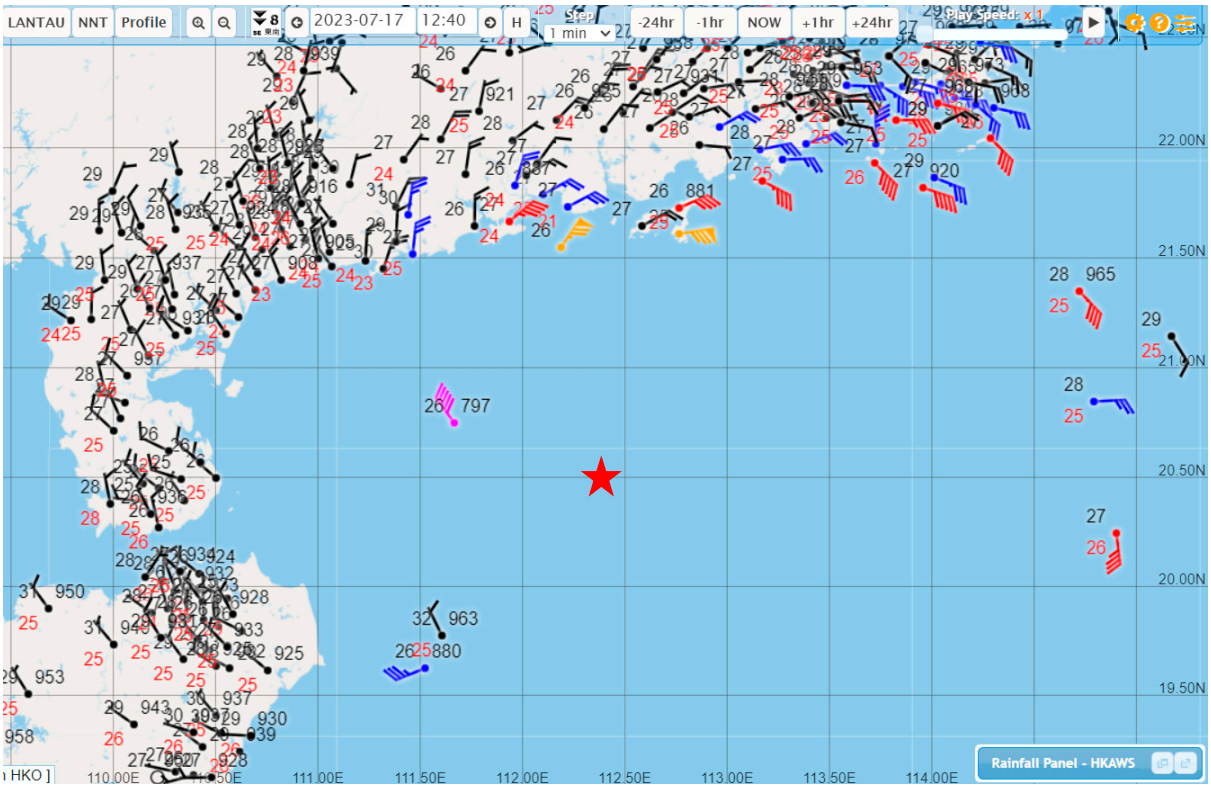

Figure 2. Surface observations at 0440 UTC 17 July 2023. The location of Talim is indicated by a red star symbol.

As an example of the radar wind profiler observations, the 925-hPa winds from the wind profilers in the region are shown in Figure 3a. The circulation of Typhoon Talim was very clear, and gale force winds were registered by a number of profilers near the Pearl River Estuary and the western coast of Guangdong. Among the profiles, the one at Xuwen (location in Figure 3a) is rather close to the centre of Talim. The profiler data (time-height cross section) is shown in Figure 3b. With the passage of the cyclone, the low level winds changed from northwesterly to southwesterly. Before the change of the wind direction, a jet of hurricane force wind was observed within the atmospheric boundary layer. This profiler is able to measure the winds up to around 16 km and thus provides valuable information of the vertical structure of Talim.

Preprints (www.preprints.org) | NOT PEER-REVIEWED | Posted: 9 August 2023 doi:10.20944/preprints202308.0713.v1

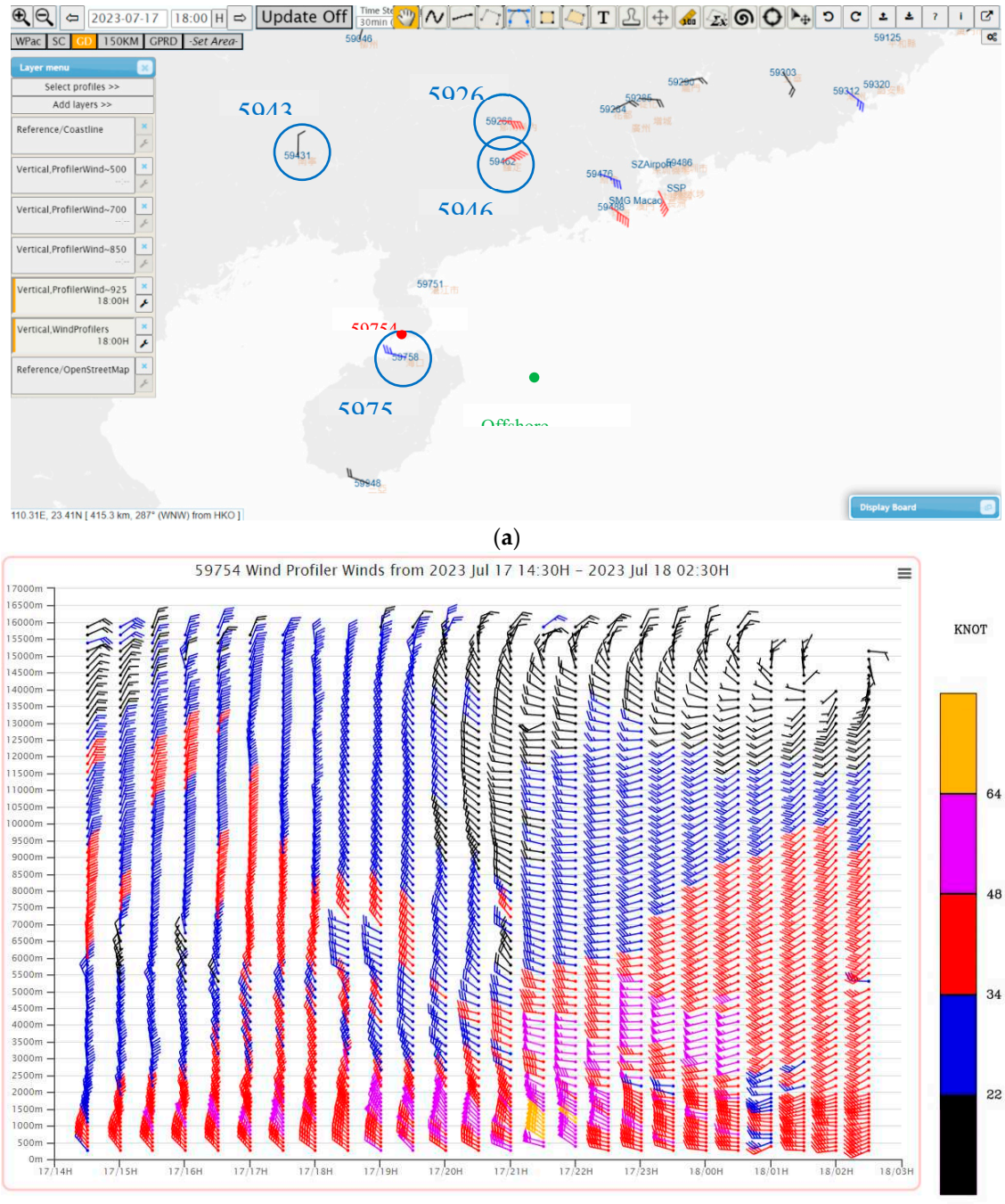

Figure 3. (**a**) 925-hPa winds from the wind profilers at 1000 UTC 17 July 2023, with the location of the wind profilers of stations 59268, 59431 Nanning, 59462 Ludong and 59758 Haikou are highlighted in blue circles. The location of wind profiler at station 59754 Xuwen at 20.24 °N, 110.16 °E and an offshore platform at 19.65 °N, 112.11 °E over the south China coastal waters are indicated by a red dot and a green dot respectively; and (**b**) time series of radar wind profiler observations at station 59754 (Xuwen) from 0630 UTC to 1830 UTC 17 July 2023. Yellow wind barbs indicated that hurricane force winds (>= 64 knots).

Radar wind profiler data analysis

The vertical wind profiles measured by the Xuwen profiler are analyzed further in Figure 4. Different stratifications of wind speeds were tried out, e.g., based on the 270-m wind for different wind speed classes (Figure 4a), and the distance from the centre of Talim (Figure 4b). It could be seen that, at relatively higher wind speed (e.g., above around 15 m/s at a height of 270 m) and for both

Preprints (www.preprints.org) | NOT PEER-REVIEWED | Posted: 9 August 2023 doi:10.20944/preprints202308.0713.v1

eyewall and outer circulation, there is a clear signature of the low level jet, with a height of around 500 m to 1000 m above the sea surface. This would have important implications for the design of wind code for tall buildings in the region to withstand the strong winds associated with tropical cyclones. For the wind direction (Figure 4b), there was clockwise rotation of the wind below 2000 m or so and then anticlockwise rotation aloft between 2000 m and 4000 m. The veering of winds would have important applications in wind engineering as well (such as Weerasuriya et al. (2018)).

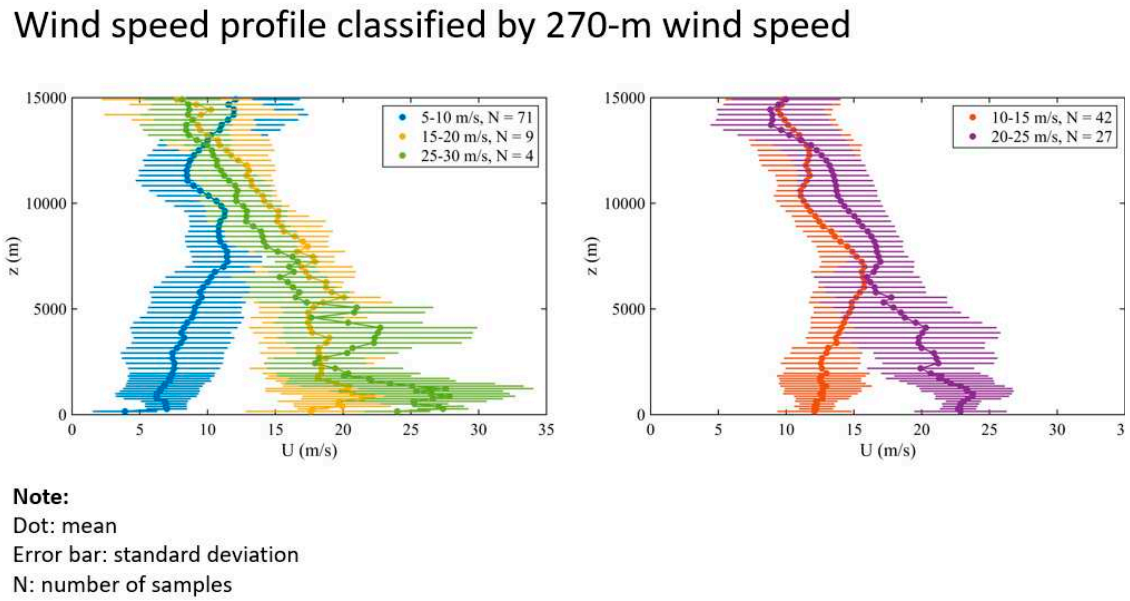

(**a**)

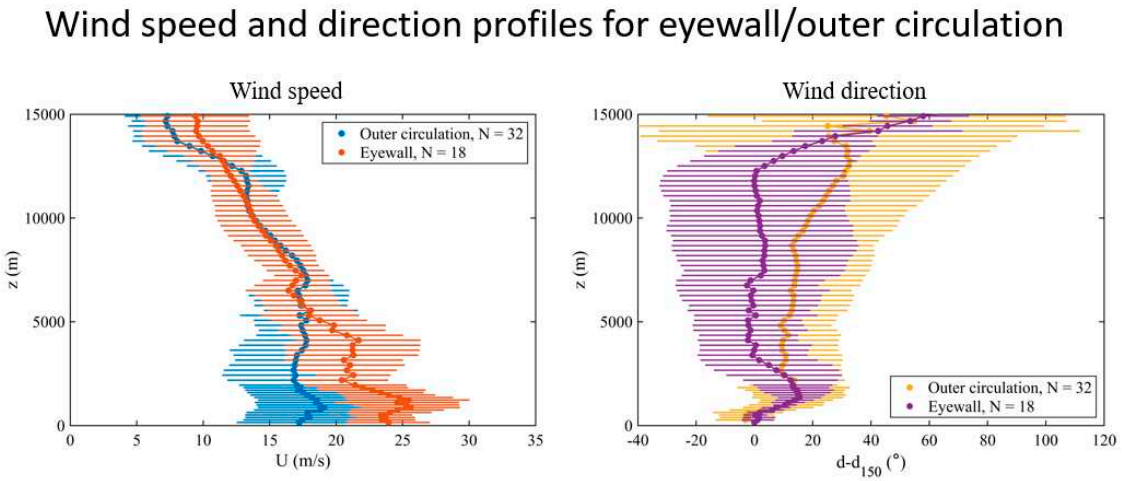

(**b**)

Figure 4. Vertical wind profiles at Xuwen stratified by (a) 270-m wind speed; and (b) distance from the centre of Talim during 0000-0900 UTC 17 July 2023 and 1800 UTC 17 July–0100 UTC 18 July 2023.

Preprints (www.preprints.org) | NOT PEER-REVIEWED | Posted: 9 August 2023 doi:10.20944/preprints202308.0713.v1

The wind speed profiles below 1000 m were fitted to the log law and power law in Figure 5 based on different stratifications of wind speeds. In general, such laws are reasonably good to describe the vertical wind profiles.

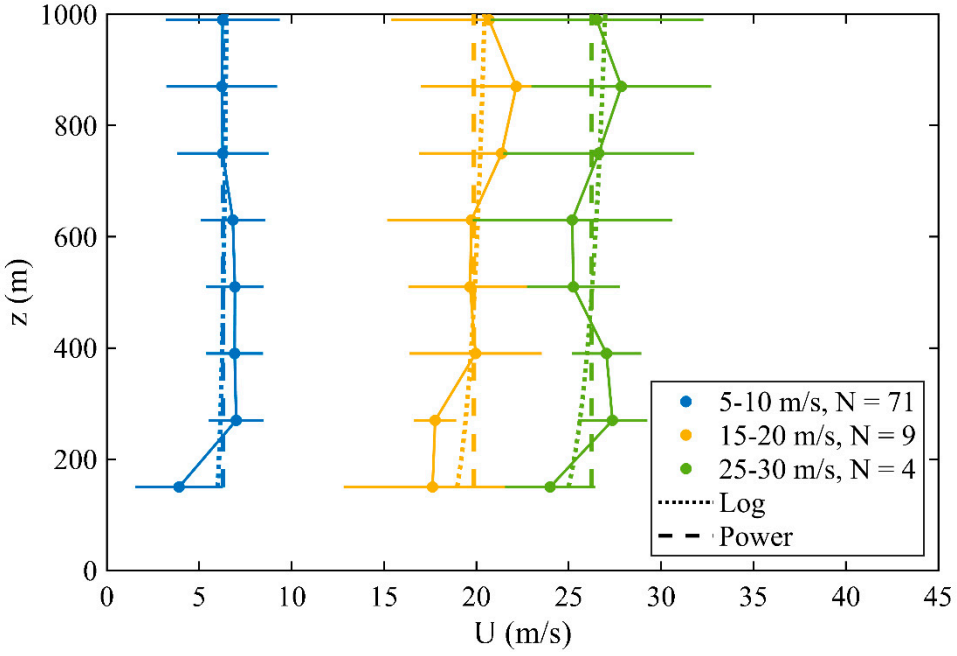

(**a**)

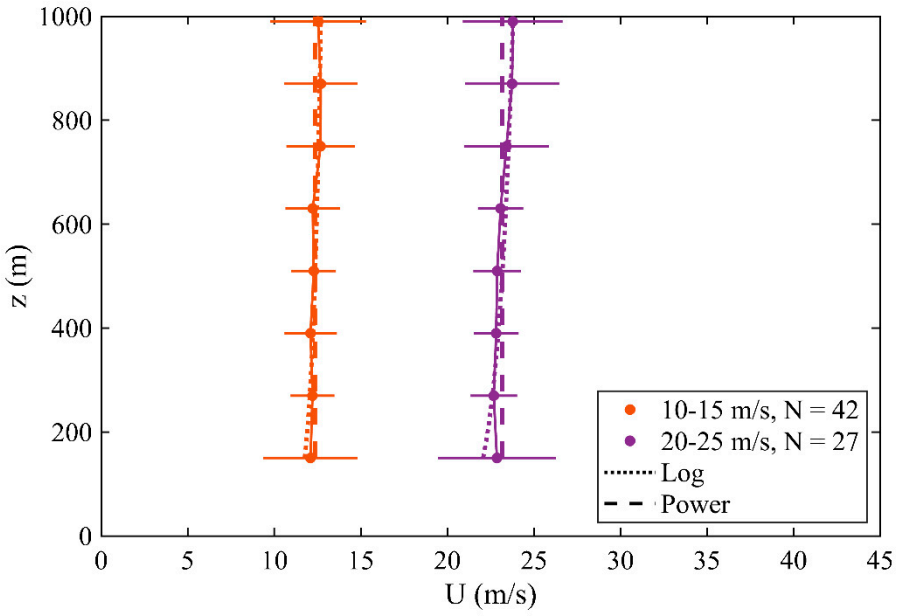

(**b**)

Figure 5. Wind speed profiles below 1000 m fitted with log law and power law based on different stratifications of wind speeds at Xuwen.

Apart from the Xuwen profiler, the vertical wind profiles of Talim have also been analysed by using a number of other radar wind profiles. Figure 6 shows the results of the station 59268 and the station 59431 Nanning (locations in Figure 3a). Similar to the Xuwen profiler, there are clear

Preprints (www.preprints.org) | NOT PEER-REVIEWED | Posted: 9 August 2023 doi:10.20944/preprints202308.0713.v1

signatures of the occurrence of a low level jet at a height of around 1000 m. The wind speed profile below 1000 m has also been analyzed (Figure 7). The log law and the power law are found to have described the vertical variation of winds rather well. As for the wind direction, winds generally rotate clockwise with height, not just within the atmospheric boundary layer but extending to a height of around, say, 6000 m or even 15000 m based on the wind profiler data from the station 59268 and the station 59462 Luoding (Figure 8). As a result, based on various wind profiler data, veering of winds with height is an important feature of the wind field of tropical cyclones for wind engineering applications.

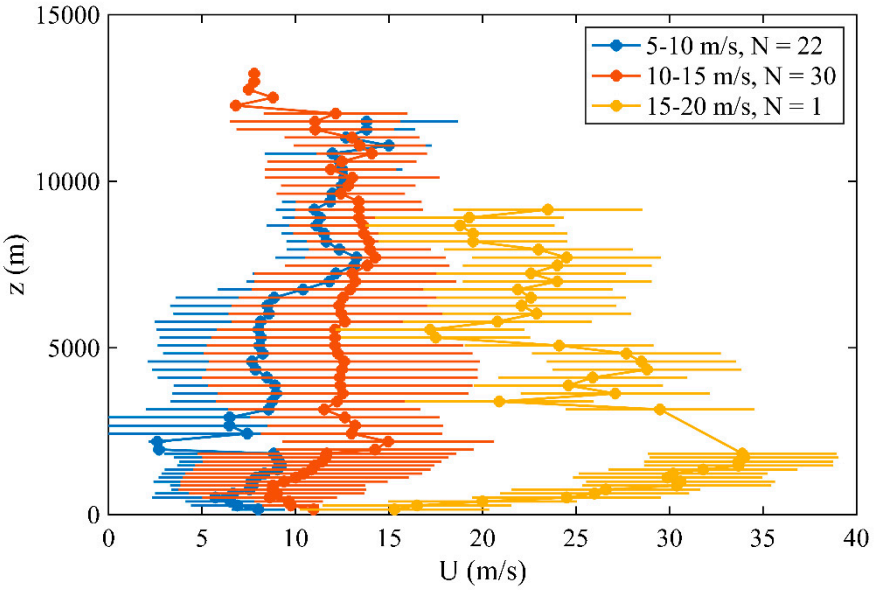

(**a**) Station 59268

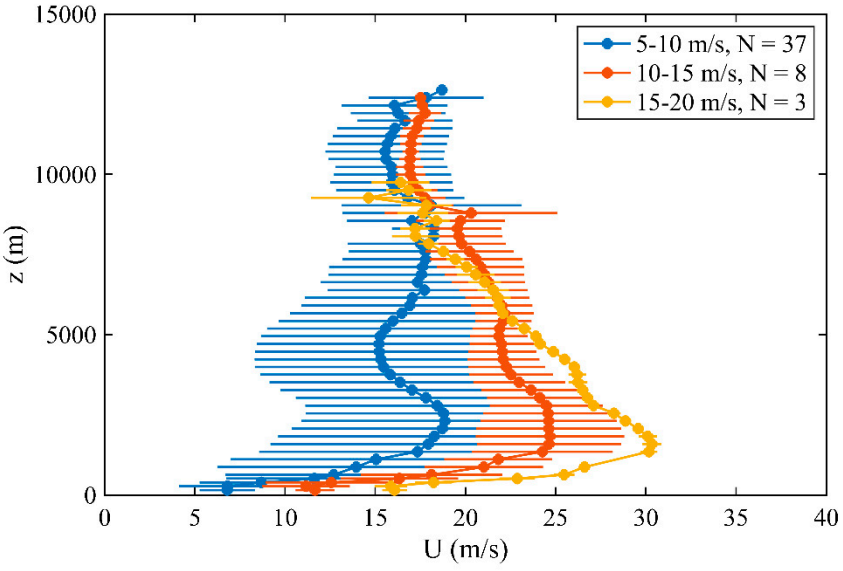

(**b**) Station 59431 Nanning

Figure 6. Similar to Figure 4a, but at (a) station 59268; and (b) station 59431 Nanning.

Preprints (www.preprints.org) | NOT PEER-REVIEWED | Posted: 9 August 2023 doi:10.20944/preprints202308.0713.v1

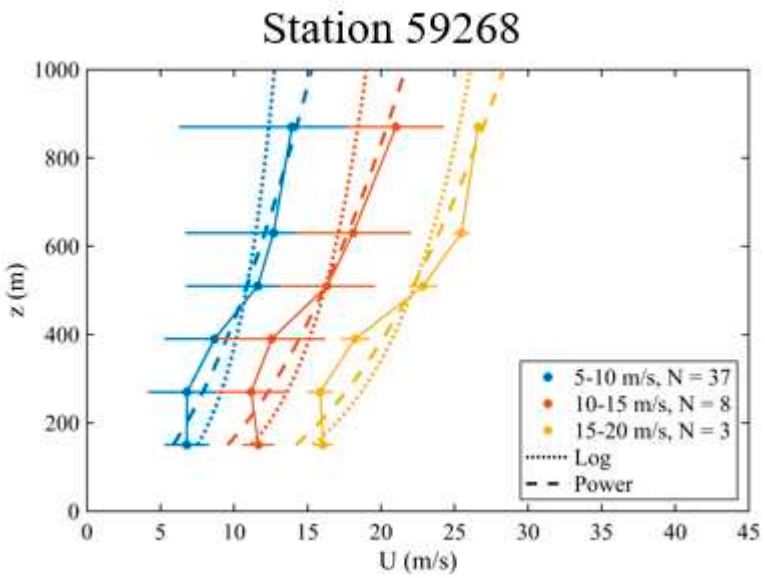

(**a**)

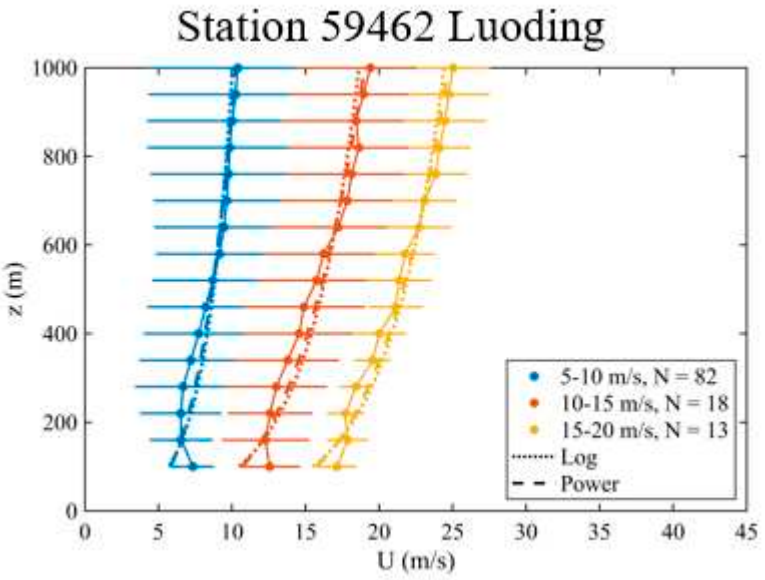

(**b**)

Figure 7. Similar to Figure 5, but at (a) station 59268; and (b) station 59462 Luoding.

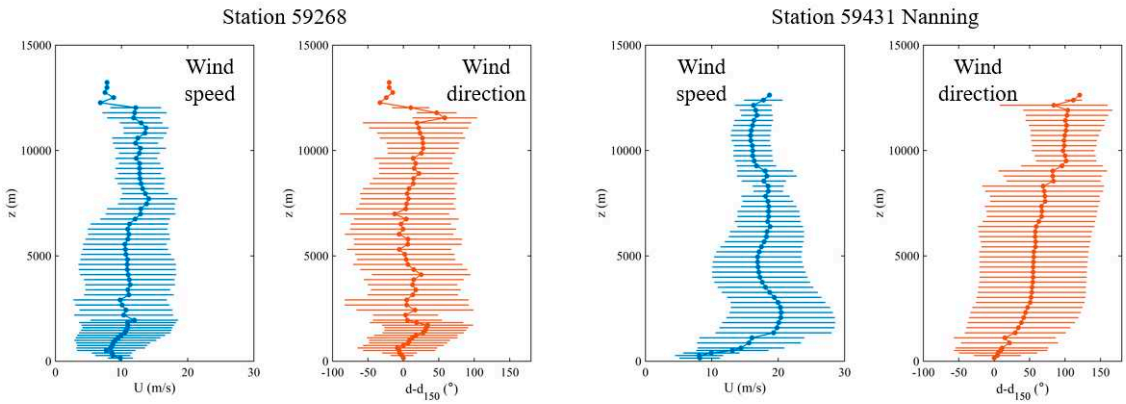

Preprints (www.preprints.org) | NOT PEER-REVIEWED | Posted: 9 August 2023 doi:10.20944/preprints202308.0713.v1

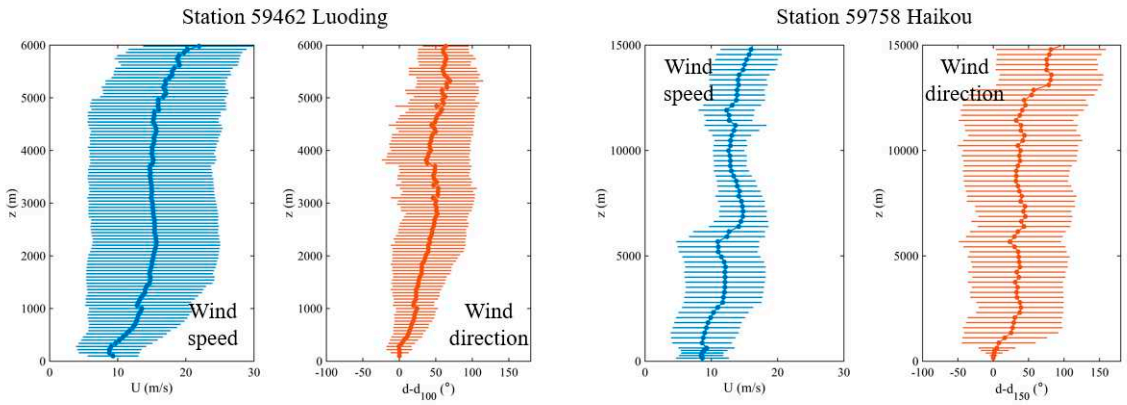

Figure 8. Similar to Figure 4a, but at station 59268, station 59431 Nanning, station 59462 Luoding and station 59758 Haikou.

LIDAR wind profiler data analysis

There is a LIDAR wind profiler on an offshore platform (location in Figure 3a) over the south China coastal waters. This instrument provides valuable information about the vertical wind profile over the sea. The analysis results of the vertical wind profile within the atmospheric boundary layer are given in Figure 9. Again, with and without the wind speed stratification (based on the wind speed at a height of 250 m), the log law and the power law fit the wind speed profiles rather well. The wind direction generally shows veering of winds with height, which is consistent with the radar wind profiler observations.

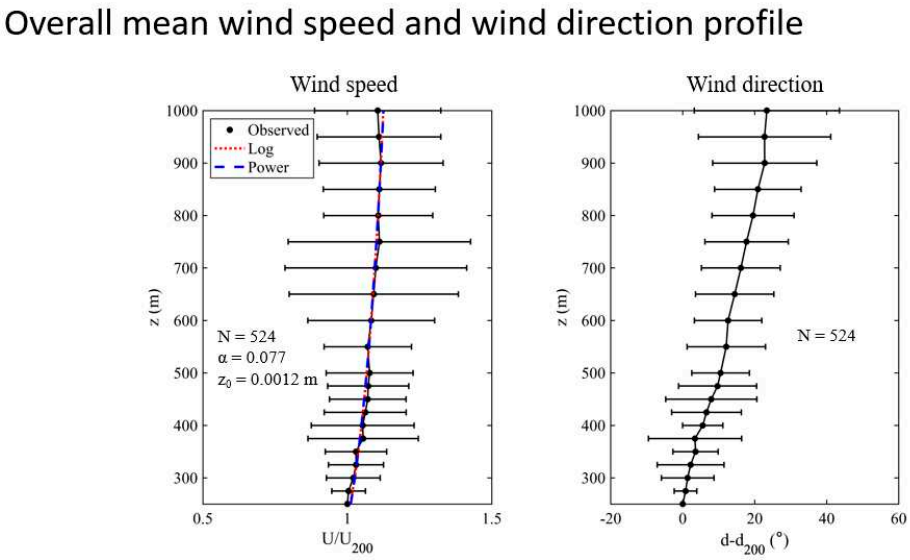

Note:
Dot: mean; Error bar: standard deviation; N: number of samples; α: power law exponent; z_0:roughness length
Only wind profile samples with 250-m wind speed larger than 5 m/s during the typhoon passage are included in the anal

(**a**)

Preprints (www.preprints.org) | NOT PEER-REVIEWED | Posted: 9 August 2023 doi:10.20944/preprints202308.0713.v1

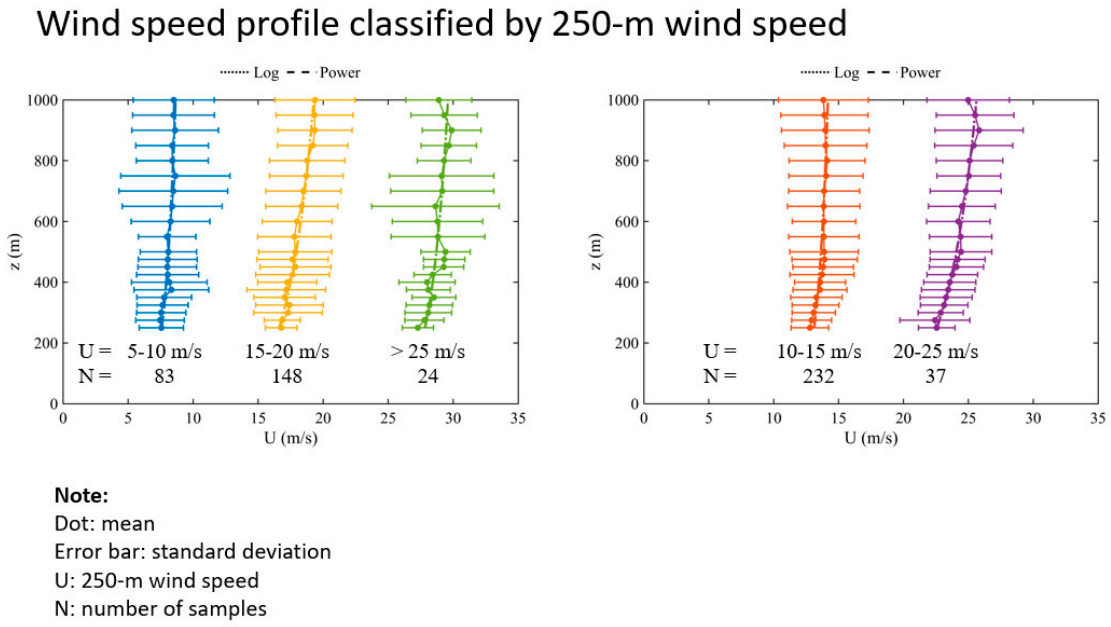

(**b**)

Figure 9. Similar to Figure 5, but over an offshore platform at 19.65 °N, 112.11 °E over the south China coastal waters.

The roughness length and the power law exponent for various wind speed ranges have been determined from the fitting of the profiles and they are summarized in Table 1. In general, alpha is in the order of 0.1, which may be expected over the open sea. The information is valuable for wind engineering applications in the south China coastal waters.

Table 1. Variation of fitted z_0 and α with 250-m wind speed.

Wind speed (m/s)	z_0 (m)	α
5-10	0.013	0.093
10-15	$1.1*10^{-5}$	0.056
15-20	0.046	0.108
20-25	0.010	0.092
>25	$9.3*10^{-8}$	0.044

Dropsonde data analysis

As in He et al. (2022), the dropsonde data have been analyzed by considering the radial/tangential flow and the equivalent potential temperature profiles. Dropsondes were launched on two days, namely, 16 and 17 July 2023. The results are summarized in Figures 10–13.

For the radial flow, inflow is not apparent in the atmospheric boundary layer from the dropsonde launch of 16 July 2023 (Figure 10). On the following day, a limited number of dropsondes show inflow on the western and southern sides of Talim, which may be related to the prevalence of the southwest monsoon (Figure 11). In general, there is not much inflow within the atmospheric boundary layer that supports rapid intensification of Talim in the study period.

Preprints (www.preprints.org) | NOT PEER-REVIEWED | Posted: 9 August 2023 doi:10.20944/preprints202308.0713.v1

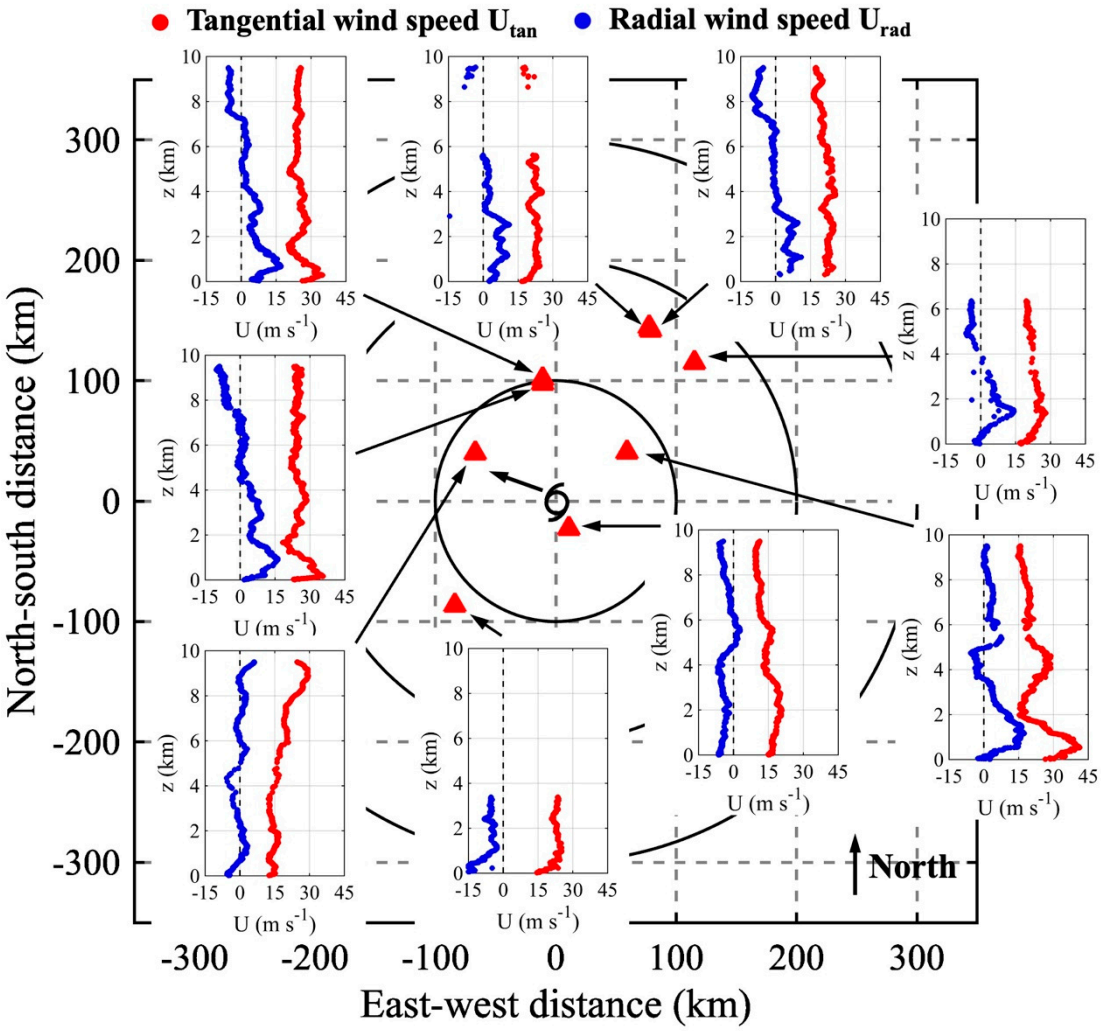

Figure 10. Vertical profiles of tangential (red) and radial (blue) wind speeds of Typhoon Talim at 0700UTC 16 July 2023. Tangential wind speed: anti-clockwise positive; radial wind speed: outflow positive. Red triangles represent dropsonde locations relative to the storm centre.

Preprints (www.preprints.org) | NOT PEER-REVIEWED | Posted: 9 August 2023 doi:10.20944/preprints202308.0713.v1

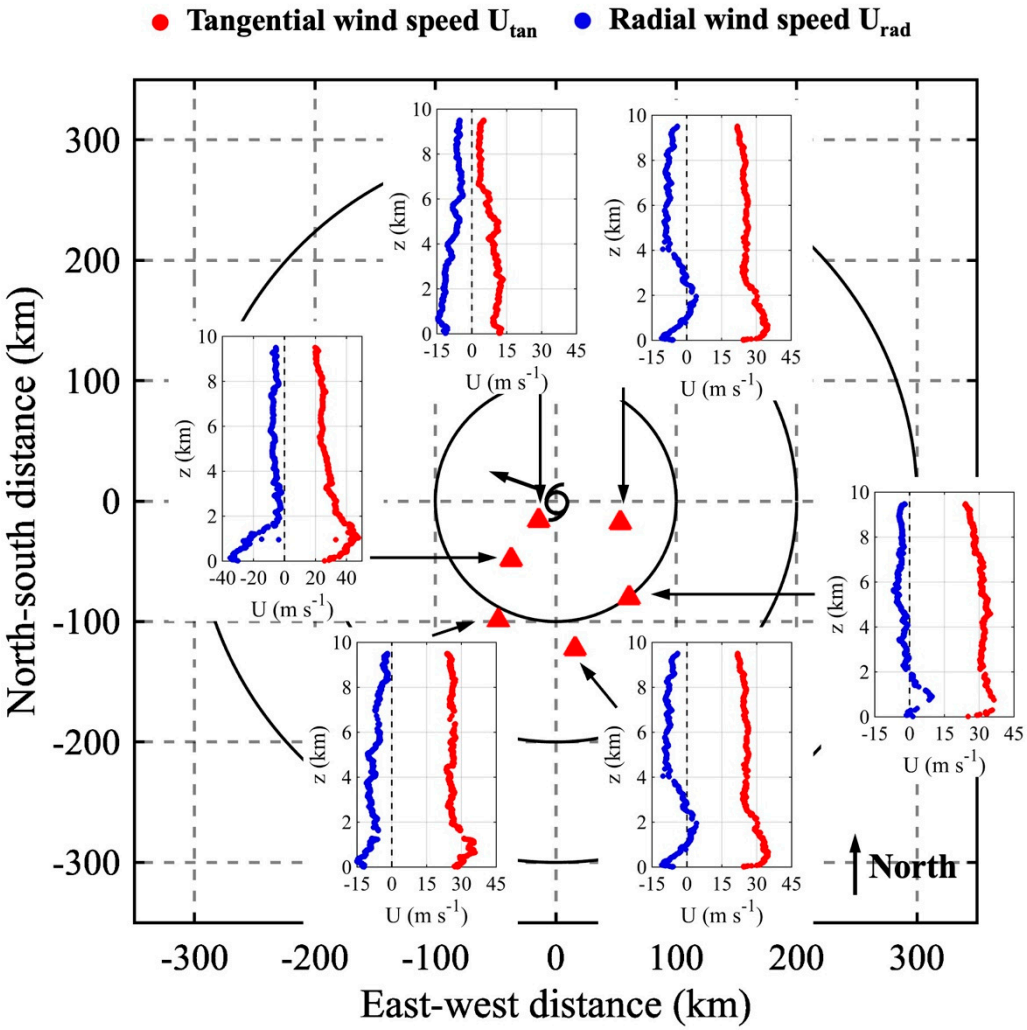

Figure 11. Vertical profiles of tangential (red) and radial (blue) wind speeds of Typhoon Talim at 0200UTC 17 July 2023. Tangential wind speed: anti-clockwise positive; radial wind speed: outflow positive. Red triangles represent dropsonde locations relative to the storm centre.

For the equivalent potential temperature profiles on the two days (Figures 12 and 13), there is a slight sign of instability of the atmospheric boundary layer, but the theta-e does not fall with height rapidly within the first 2 km or so above the sea surface. Again, this is consistent with the meteorological satellite observation that Talim was not intensifying rapidly during the period.

Preprints (www.preprints.org) | NOT PEER-REVIEWED | Posted: 9 August 2023 doi:10.20944/preprints202308.0713.v1

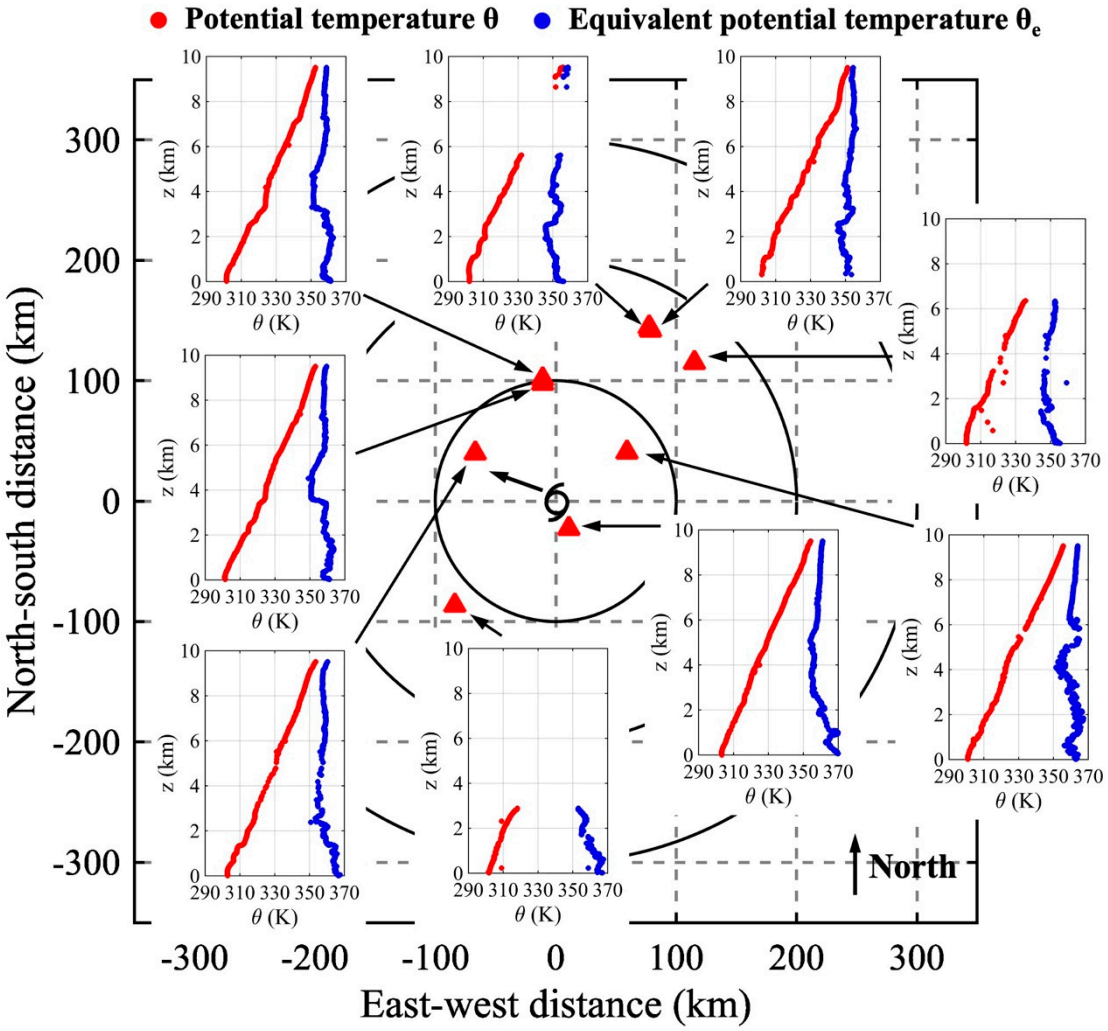

Figure 12. Vertical profiles of potential temperature (red) and equivalent potential temperature (blue) of Typhoon Talim at 0700UTC 16 July 2023. Red triangles represent dropsonde locations relative to the storm centre.

Preprints (www.preprints.org) | NOT PEER-REVIEWED | Posted: 9 August 2023 doi:10.20944/preprints202308.0713.v1

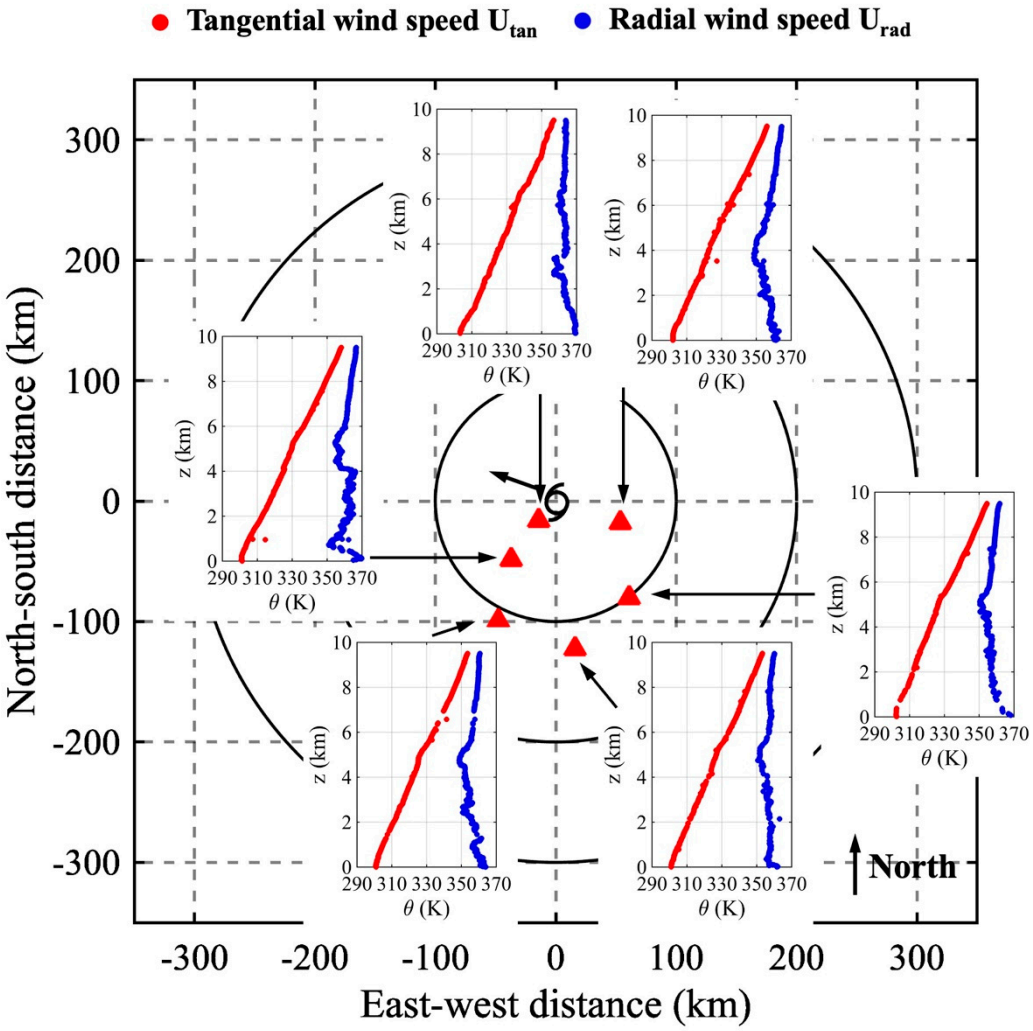

Figure 13. Vertical profiles of potential temperature (red) and equivalent potential temperature (blue) of Typhoon Talim at 0200UTC 17 July 2023. Red triangles represent dropsonde locations relative to the storm centre.

The vertical cross sections of equivalent potential temperatures are shown in Figure 14 for the two days. On the first day, below 700 hPa or so, there appears to be tilting of the cyclone centre with height, with the warm core structure not well aligned vertically (Figure 14a). The vertical alignment appears slightly better on the following day (Figure 14b). Such observations would be compared with re-analysis data from numerical weather prediction models in the future.

Preprints (www.preprints.org) | NOT PEER-REVIEWED | Posted: 9 August 2023 doi:10.20944/preprints202308.0713.v1

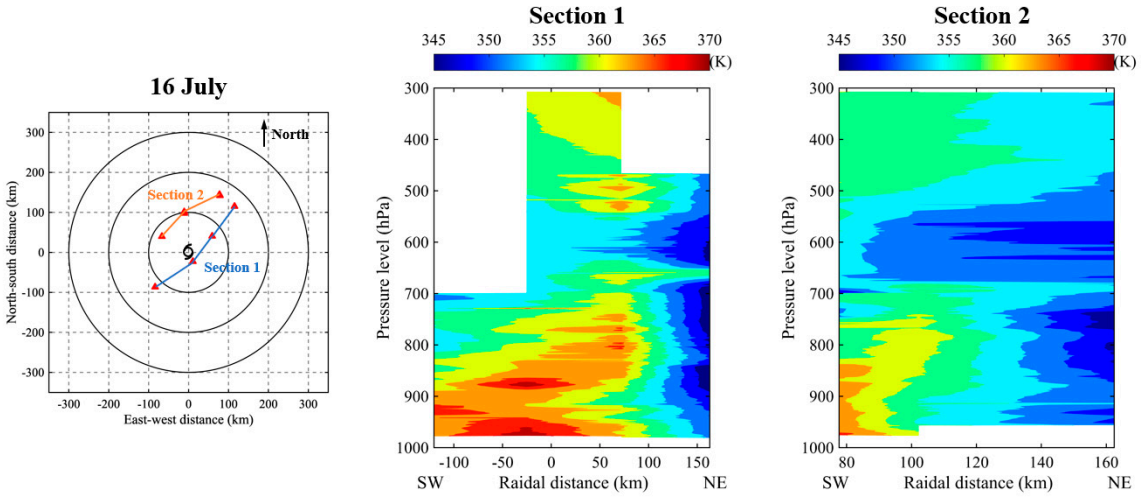

(a)

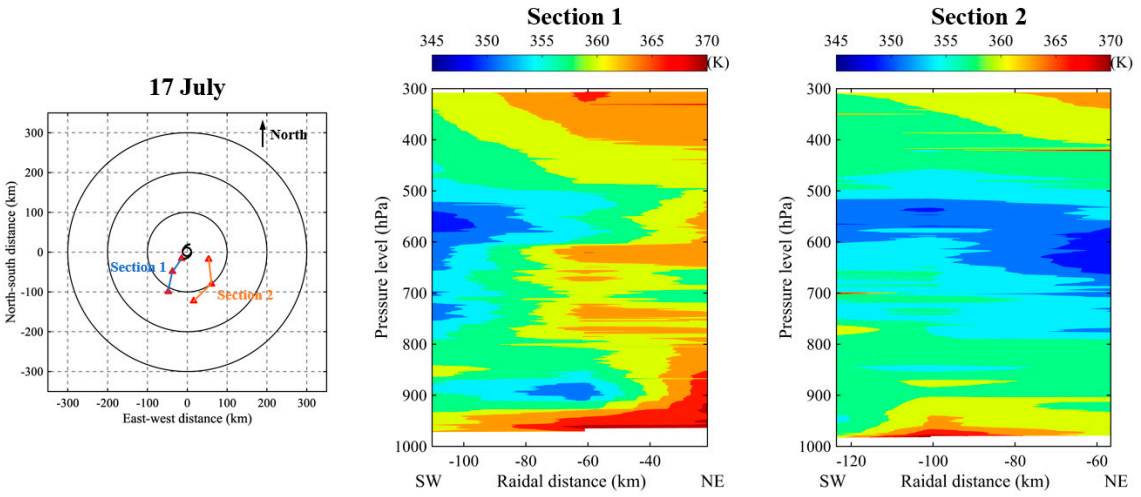

(b)

Figure 14. Vertical cross sections of equivalent potential temperatures of Typhoon Talim on (a) 16 July and (b) 17 July 2023.

The vertical wind profiles obtained from dropsondes have been fitted with the various laws in the literature and the results are shown in Figure 15. Consistent with the previous studies (e.g., He et al. (2022)) of tropical cyclones in the region, the Vickery et al. (2009) model appears to be the best in explaining the vertical variation of wind speed with height. At a distance of around 60 km from the centre of Talim, the wind speed could reach 35 m/s, which is consistent with the surface observations mentioned earlier in the paper.

Preprints (www.preprints.org) | NOT PEER-REVIEWED | Posted: 9 August 2023 doi:10.20944/preprints202308.0713.v1

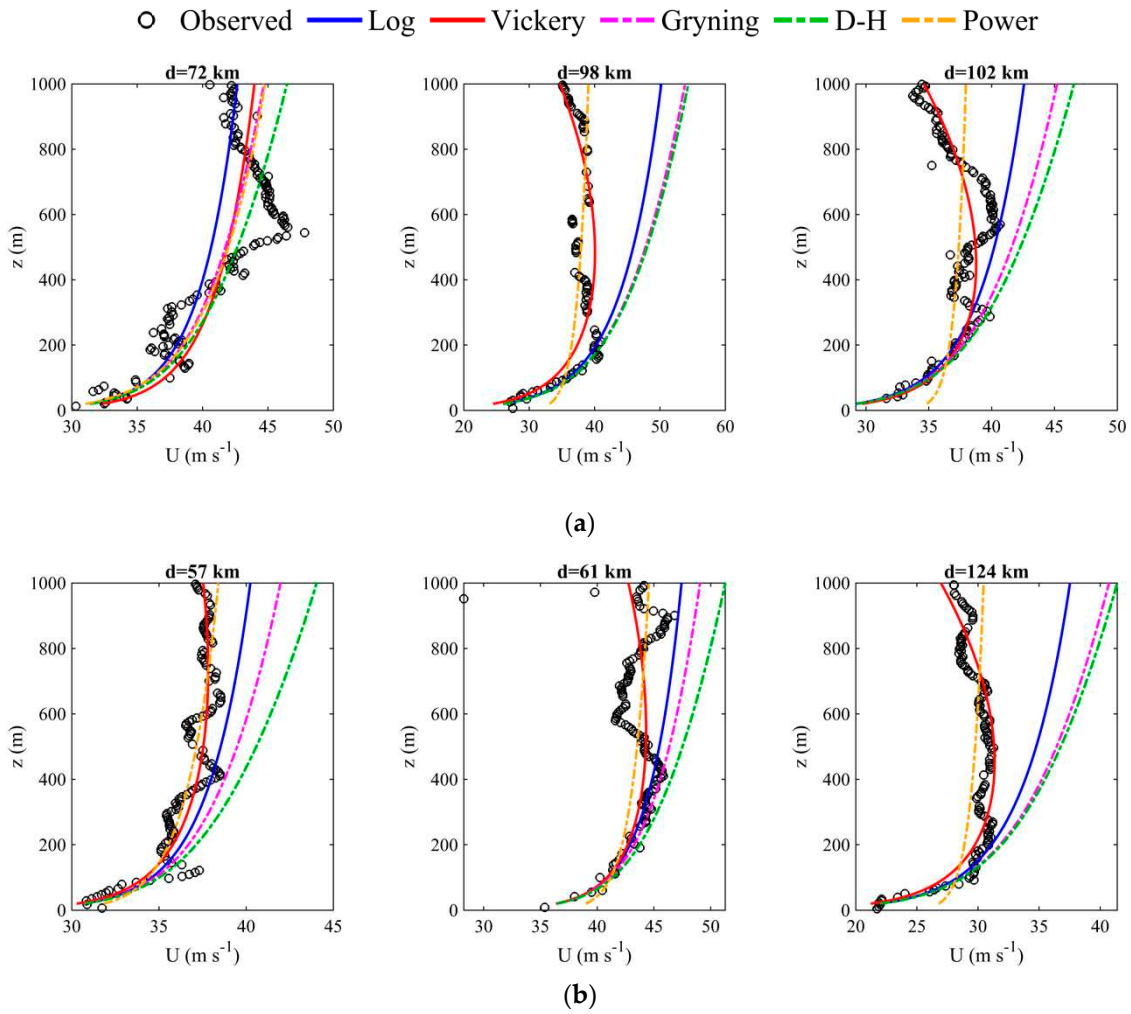

Figure 15. Fitting of selected vertical profiles of wind speeds in the lowest 1000 m near the eyewall of Typhoon Talim (a) at 0700UTC 16 July 2023 and (b) at 0200UTC 17 July 2023 to the wind profile models, including the logarithmic law, Vickery et al. (2009) model, Gryning et al. (2007) model, Deaves & Harris (1978) model, and power law. *d* represents the distance to the storm centre.

Preliminary observations from ocean radar

The first set of HF ocean radar in Hong Kong installed in 2021 and operating at 5.275 MHz at Cape D'Aguilar is paired up with another set at Shanwei operated by the South China Sea Bureau of the Ministry of Natural Resources of China. Though extracting information on winds and waves from much weaker or partial parts of the backscattered signals of the composite radar data that are easily corrupted by noise and interference presents much challenges (Barrick et al.(1977); Wyatt et al. (2006); Mantovani et al. (2020)), the derived second order measurements could sometimes provide very useful wind information and the trend of wind speed over the sea areas up to about 250 km southeast of Hong Kong. Figure 16 shows the wind speed observations from the ocean radar pair when Talim was edging closer to the south China coast on 16-17 July 2023. The observations revealed a relatively large vortex structure of Talim with a gale wind radius in the order of 250 km (deep red region in Figure 16) and a storm wind radius in the order of 180 km (purple region in the same figure) over the its northern quadrant. Storm force winds affected outlying islands south of Hong Kong including Huangmaozhou on the morning of 17 July 2023 which matched well with the extrapolation of ocean radar wind speed field. It is evident that ocean radar observations would be useful for monitoring the development of tropical cyclones near shore and nowcasting of high winds and waves over coastal areas if the wind retrieval algorithm is well tuned and the signal-to-noise ratio is sufficiently high.

Preprints (www.preprints.org) | NOT PEER-REVIEWED | Posted: 9 August 2023 doi:10.20944/preprints202308.0713.v1

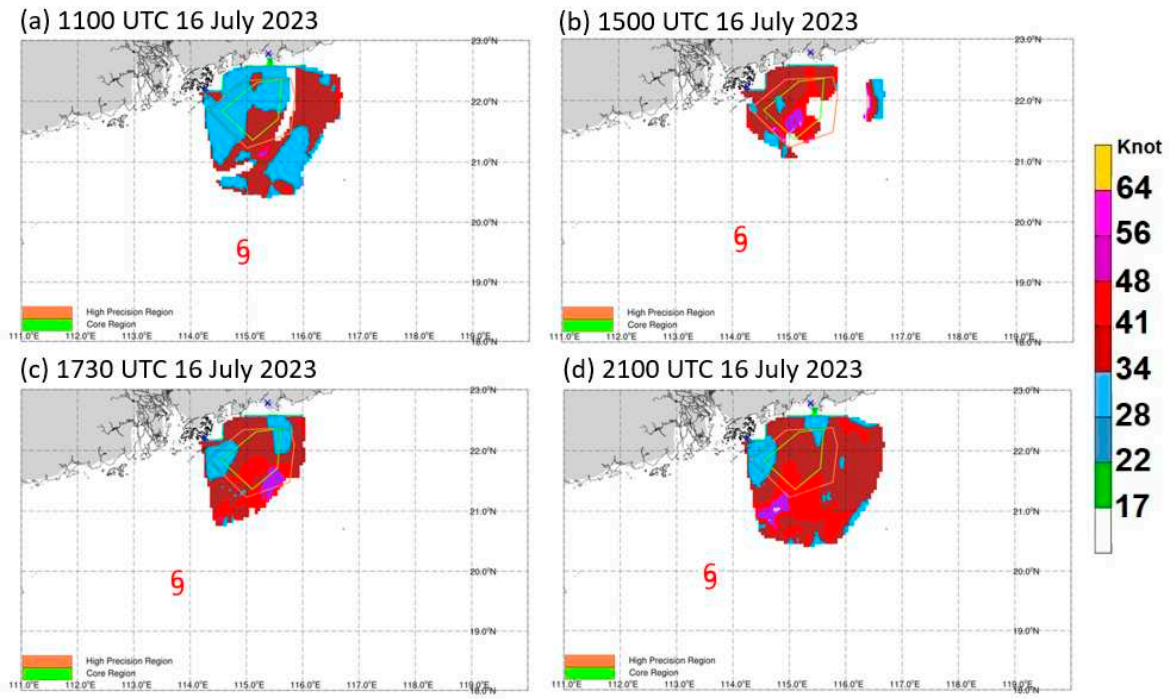

Figure 16. Wind speed observations from the ocean radar pair of Hong Kong and Shanwei. The tropical cyclone symbol marked the position of Talim as determined from surface observations and satellite fixes.

Conclusions

This paper provides a comprehensive document of the observations, both surface and upper air, for Typhoon Talim over the northern part of the South China Sea. It is confirmed from the various surface observations that Talim is indeed a typhoon. The upper air measurements show that, in the atmospheric boundary layer below 1000 m or so above sea surface, the log law and the power law fit the wind speed profile very well. A low level jet is observed from the radar wind profiler observations. The ocean radar data are also found to provide unprecedented view of the surface wind pattern associated with Talim.

More and more weather buoys and offshore wind profilers would be deployed in the region. Case studies and statistical analysis would be conducted in the future for tropical cyclones over the northern part of the South China Sea. The upper air data, in particular, would be useful for wind engineering applications.

References

1. Barrick, D.E., M.W. Evans, and B.L. Weber, 1977: Ocean surface currents mapped by radar. Science 198, 138-144. doi: 10.1126/science.198.4313.138
2. He, Junyi, K.K. Hon, P.W. Chan, and Q.S. Li, 2022: Dropsonde observations and numerical simulations of intensifying/weakening tropical cyclones over the northern South China Sea. Weather, 77, 332-338
3. Hon, Kai-kwong, and Pak Wai Chan, 2022: A decade (2011–2020) of tropical cyclone reconnaissance flights over the South China Sea. Weather, 77, 308-314
4. Mantovani, C., L. Corgnati, J. Horstmann, A. Rubio, E. Reyes, C. Quentin, S. Cosoli, J.L. Asensio, J. Mader, and A. Griffa, 2020: Best practices on high frequency radar deployment and operation for ocean current measurement. Front. Mar. Sci. 7:210. doi:10.3389/fmars.2020.00210
5. Wyatt, L.R., J.J. Green, A. Middleditch, M.D. Moorhead, J. Howarth, M. Holt, et al., 2006: Operational wave, current and wind measurements with the pisces HFR. J. Ocean Eng. 31, 819-834. doi: 10.1109/JOE.2006.888378
6. Weerasuriya, A.U., Z.Z. Hu, X.L. Zhang, K.T. Tse, S. Li, and P.W. Chan, 2018: New inflow boundary conditions for modeling twisted wind profiles in CFD simulation for evaluating the pedestrian-level wind field near an isolated building. Building and Environment 132, 303-318